Supplement of Atmos. Chem. Phys., 22, 10827–10839, 2022
https://doi.org/10.5194/acp-22-10827-2022-supplement

Atmospheric Chemistry and Physics
Open Access

Supplement of

Secondary organic aerosols from OH oxidation of cyclic volatile methyl siloxanes as an important Si source in the atmosphere

Chong Han et al.

Correspondence to: Shao-Meng Li (shaomeng.li@pku.edu.cn)

Text S1. Si/O and Si/C ratios of $C_xH_yO_zSi_n$ in D5 and D6 SOAs

The calculation processes of the Si/O and Si/C ratios at each PA are shown as follows:

(1) The normalized peak intensity of $C_xH_yO_zSi_n$ ($C_{x1}H_{y1}O_{z1}Si_{n1}$, $C_{x2}H_{y2}O_{z2}Si_{n2}$ …$C_{xi}H_{yi}O_{zi}Si_{ni}$) is obtained from the HR-ToF-AMS, which is named as A_1, A_2…A_i, respectively.

(2) The fraction of each $C_xH_yO_zSi_n$ ion (F_1, F_2, F_3…F_i) is calculated by Equation S1,

$$F_i = A_i / \mathrm{SUM}\,(A_1, A_2, A_3 \ldots A_i) \quad \text{(S1)}$$

(3) The Si/O and Si/C ratio of $C_xH_yO_zSi_n$ ions at each equivalent day are calculated by Equation S2-S6,

$$m_{Si} = \mathrm{SUM}(F_i \times n_i \times M_{Si} / M_{C_{xi}H_{yi}O_{zi}Si_{ni}}) \quad \text{(S2)}$$

$$m_O = \mathrm{SUM}(F_i \times z_i \times M_O / M_{C_{xi}H_{yi}O_{zi}Si_{ni}}) \quad \text{(S3)}$$

$$m_C = \mathrm{SUM}(F_i \times x_i \times M_C / M_{C_{xi}H_{yi}O_{zi}Si_{ni}}) \quad \text{(S4)}$$

$$n/z = \frac{m_{Si}}{M_{Si}} \Big/ \frac{m_O}{M_O} \quad \text{(S5)}$$

$$n/x = \frac{m_{Si}}{M_{Si}} \Big/ \frac{m_C}{M_C} \quad \text{(S6)}$$

where M is the molar mass of one specific element (Si, O, C and H) or $C_xH_yO_zSi_n$ ions; m is the total mass of Si, O or C in all $C_xH_yO_zSi_n$ ions. For the calculation results, there may be some uncertainties due to the assignments of peaks in the HR-ToF-AMS and the fragmentation processes of the AMS ionization (Aiken et al., 2007).

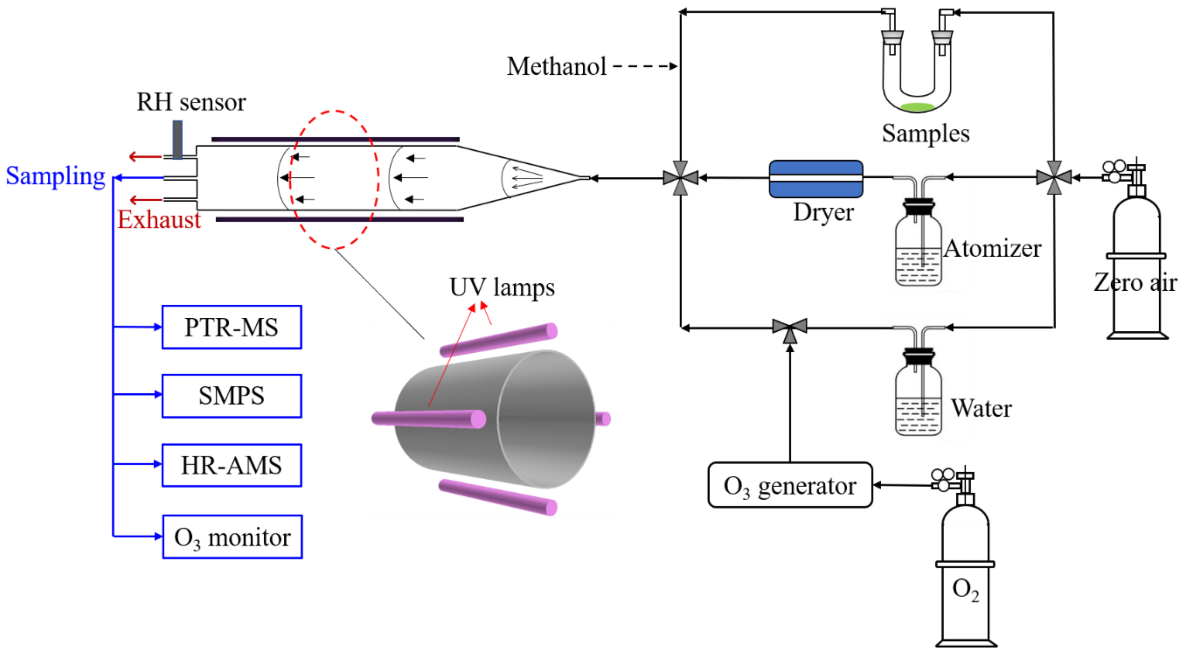

Figure S1. Details of experimental setup

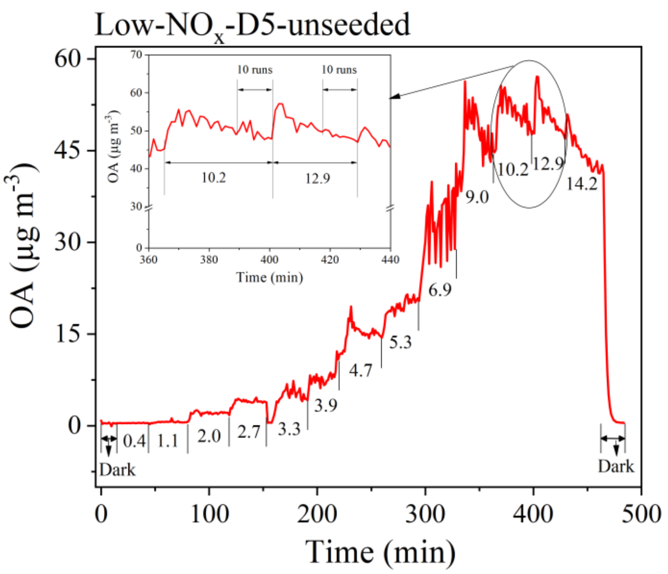

Figure S2. The AMS time series of D5 SOAs in low-NO_x experiments under unseeded conditions. The numbers represent the equivalent photochemical age, and the inset is an enlarged view at 10.2 and 12.9 PA.

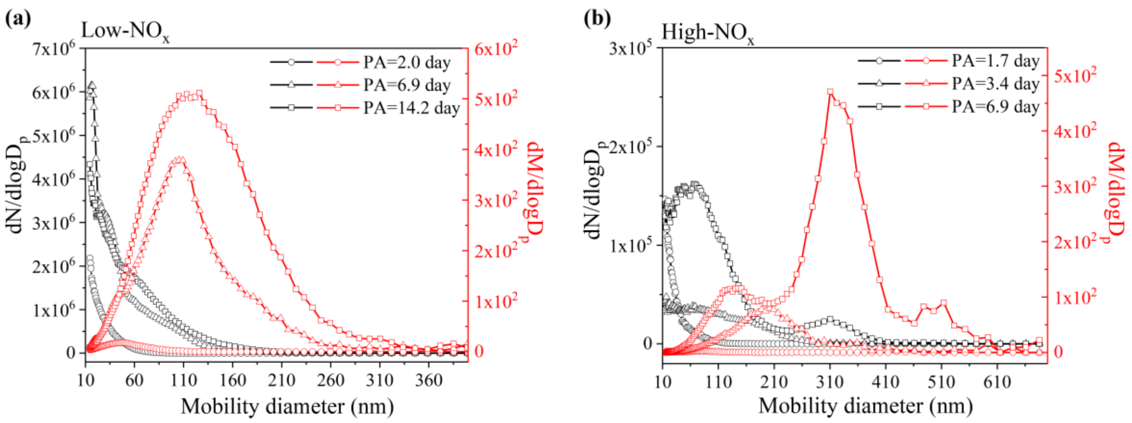

Figure S3. Number and mass size distributions of D5 SOAs measured by SMPS under (**a**) low-NO_x (PA=2.0, 6.9 and 14.2 days) and (**b**) high-NO_x (PA=1.7, 3.4 and 6.9 days) conditions.

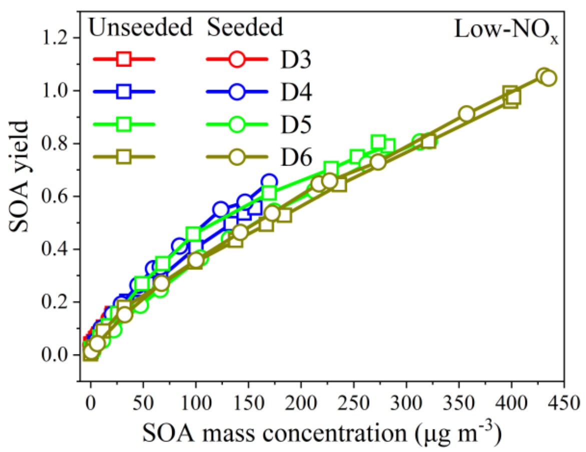

Figure S4. The relationship between SOA yields and mass concentration for cVMSs in low-NO_x experiments.

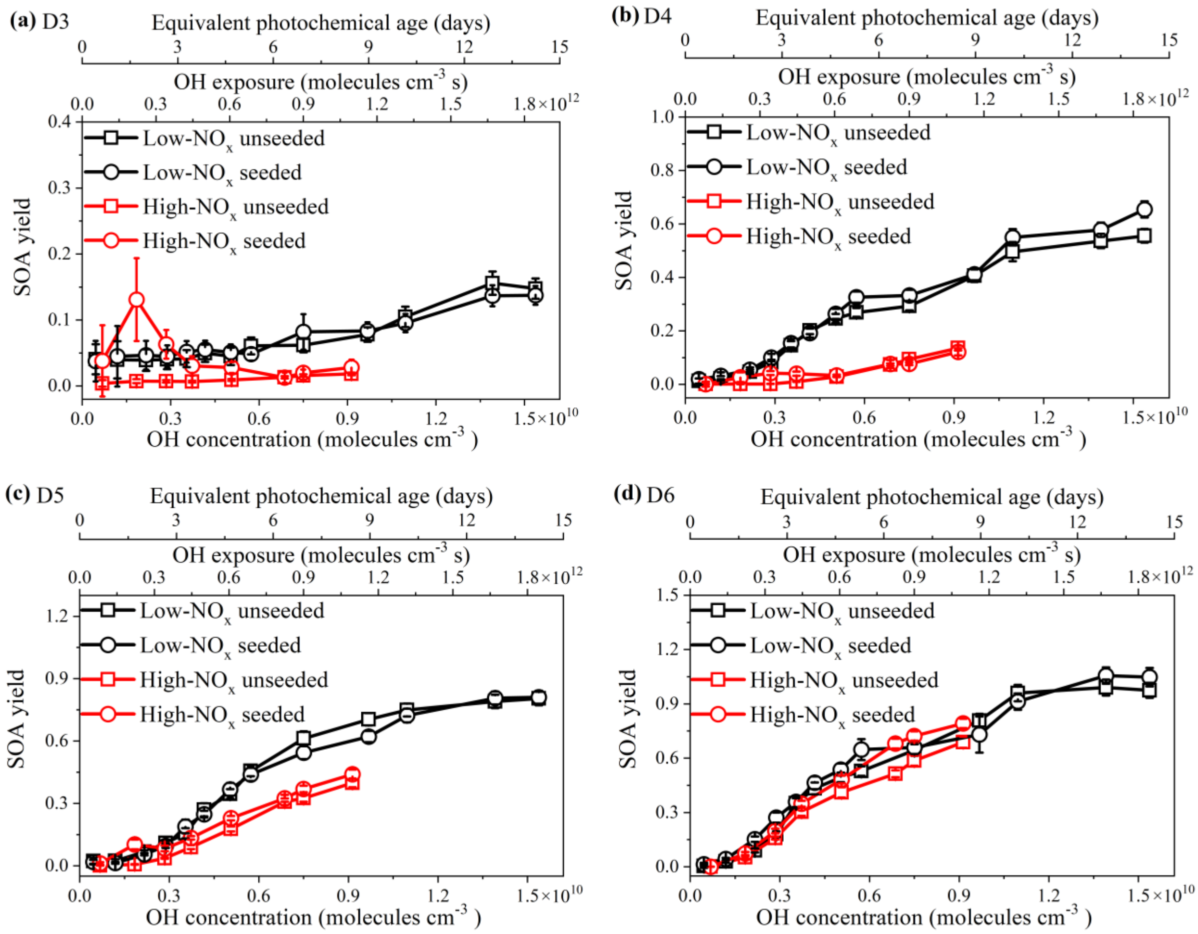

Figure S5. Comparison of low-NO_x (black) and high-NO_x (red) SOA yields for cVMSs (**a-d**) for unseeded (square symbols) and seeded (circular symbols) experiments.

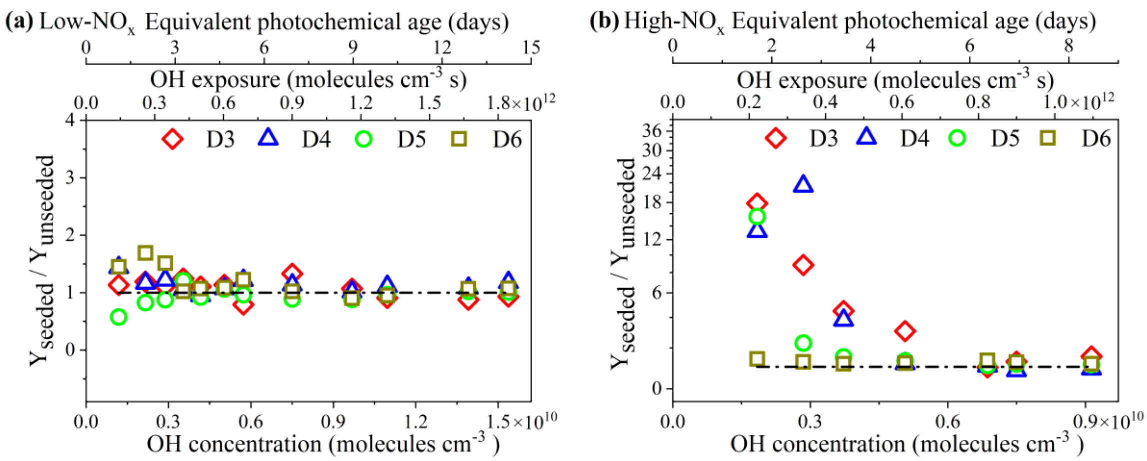

Figure S6. SOA yield enhancement ratio ($Y_{seeded}/Y_{unseeded}$) in the presence of seed particles. (**a**) Low-NO_x experiments; (**b**) high-NO_x experiments. The dotted lines represent $Y_{seeded}/Y_{unseeded}$=1.

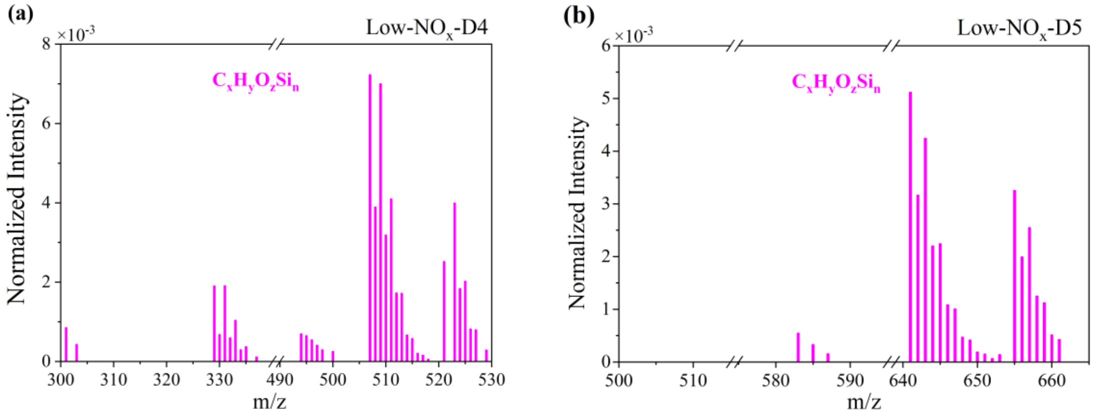

Figure S7. HR-ToF-AMS mass spectra of D4 (**a**) and D5 (**b**) in high m/z range at OH exposure of 9.0×10^{11} molecules cm^{-3} s (i.e., OH concentration of 7.5×10^{9} molecules cm^{-3}) under low-NO_x conditions in unseeded experiments.

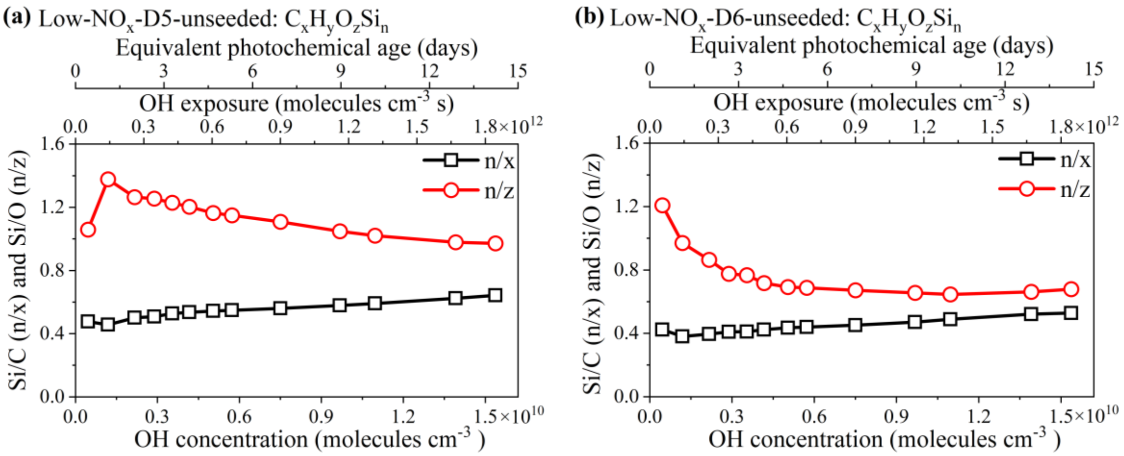

Figure S8. The weighted average values of Si/C (n/x) and Si/O (n/z) ratios for $C_xH_yO_zSi_n$ groups in SOAs derived from the oxidation of D5 (**a**) and D6 (**b**) by OH radicals at different photochemical ages under low-NO_x and unseeded conditions.

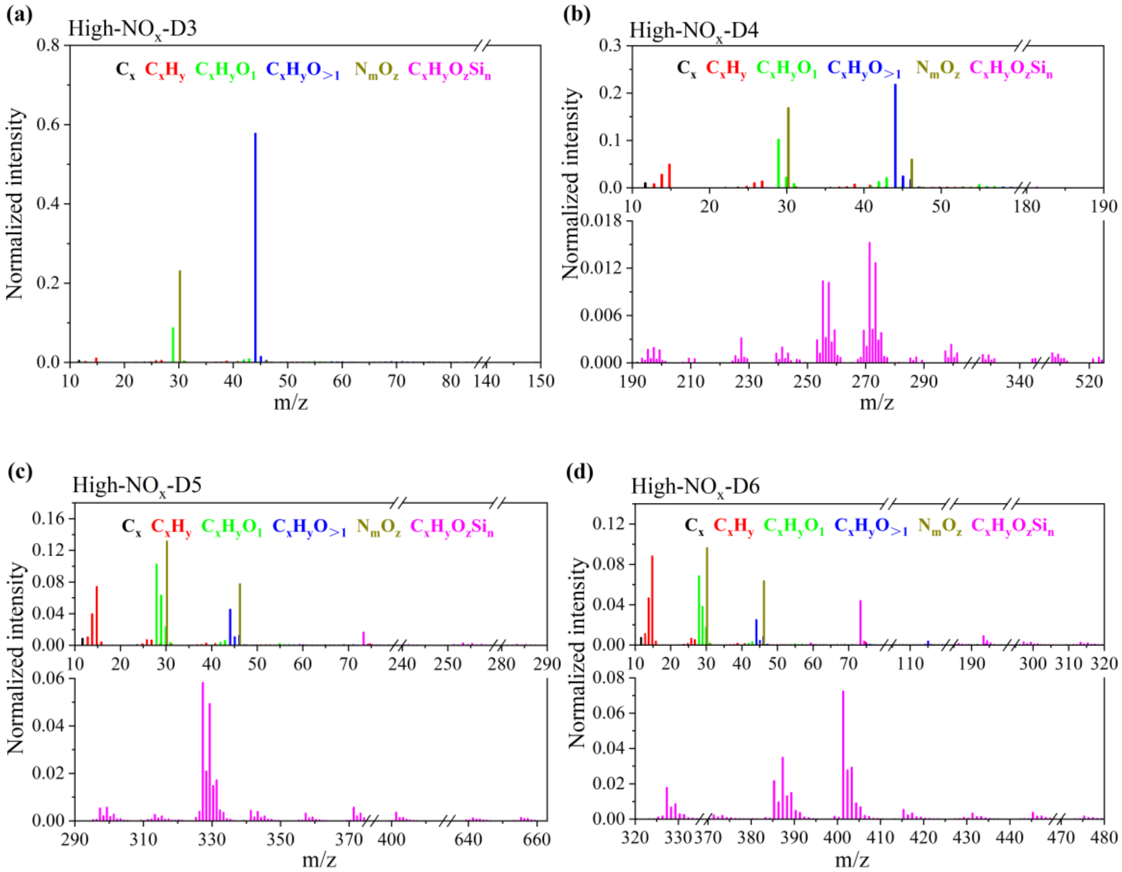

Figure S9. HR-ToF-AMS mass spectra of cVMS SOAs at OH exposure of 9.0 × 10^{11} molecules cm^{-3} s (i.e., OH concentration of 7.5 × 10^{9} molecules cm^{-3}) under high-NO_x conditions in unseeded experiments. (**a-d**) represent data of D3-D6, respectively.

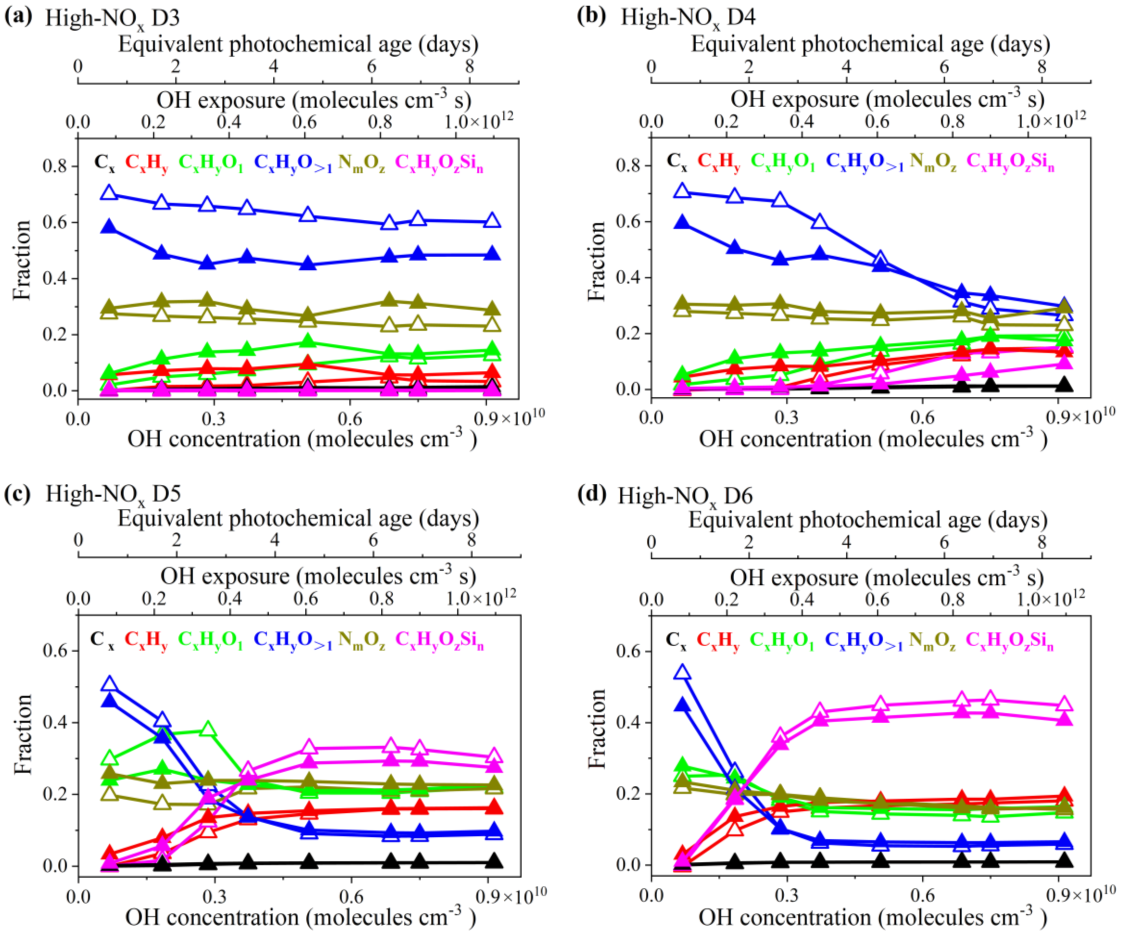

Figure S10. Fraction of C_x, C_xH_y, $C_xH_yO_1$, $C_xH_yO_{>1}$ and $C_xH_yO_zSi_n$ groups for SOAs derived from the oxidation of cVMSs (**a-d**) by OH radicals at different photochemical ages under high-NO_x conditions. Empty and solid triangles represent experimental data under unseeded and seeded conditions, respectively.

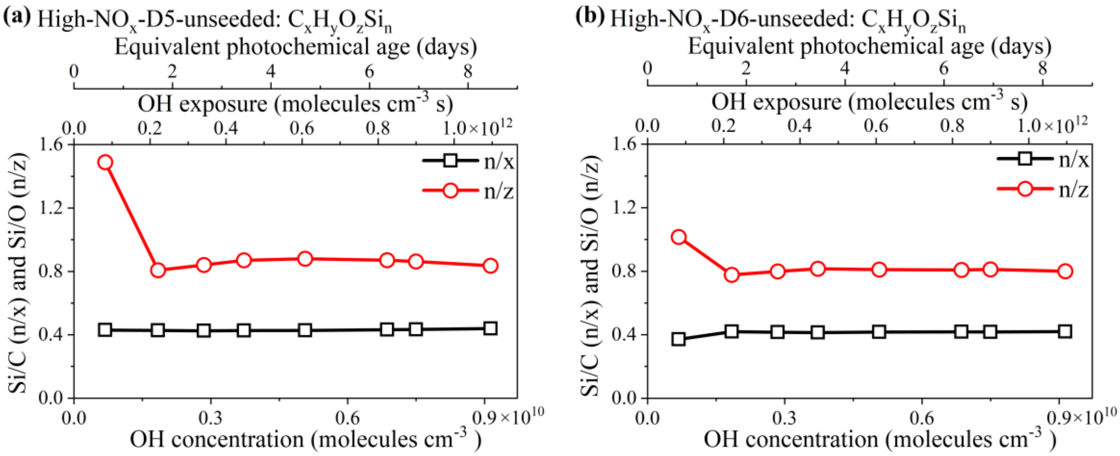

Figure S11. The weighted average values of Si/C (n/x) and Si/O (n/z) ratios for $C_xH_yO_zSi_n$ groups in SOAs derived from the oxidation of D5 (**a**) and D6 (**b**) by OH radicals at different photochemical ages under high-NO_x and unseeded conditions.

Table S1. Formula and structures of cyclic volatile methyl siloxanes

Name and Abbreviation	Formula	Structure
Hexamethylcyclotrisiloxane (D3)	$C_6H_{18}O_3Si_3$	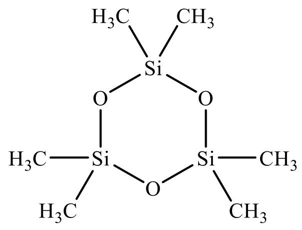
Octamethylcyclotetrasiloxane (D4)	$C_8H_{24}O_4Si_4$	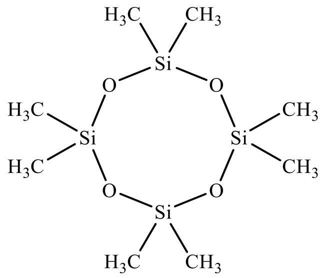
Decamethylcyclopentasiloxane (D5)	$C_{10}H_{30}O_5Si_5$	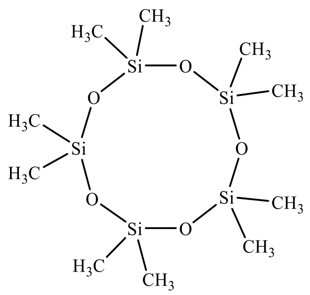
Dodecamethylcyclohexasiloxane (D6)	$C_{12}H_{36}O_6Si_6$	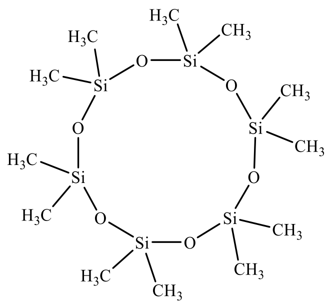

Table S2. The concentration of cVMSs at the reactor inlet and outlet.

cVMSs	Low-NO_x experiment (ppb)		High-NO_x experiment (ppb)	
	unseeded	seeded	unseeded	seeded
$[D3]_i$	19.91	20.06	41.20	42.90
$[D3]_o$	3.28	3.14	13.03	14.76
$[D4]_i$	30.89	29.83	27.05	28.56
$[D4]_o$	4.87	4.51	5.95	7.08
$[D5]_i$	21.51	28.45	38.50	35.99
$[D5]_o$	0	0.12	7.31	7.39
$[D6]_i$	24.40	27.08	26.92	28.67
$[D6]_o$	1.23	1.16	5.73	6.03

Note: 'i' and 'o' means the reactor inlet and outlet, respectively; the OH exposure is 1.85×10^{12} and 1.10×10^{12} molecules cm^{-3} s in low and high-NO_x experiments, respectively.

Table S3. Background data of SMPS at different OH exposures in low and high-NO_x experiments without cVMSs.

Low-NO_x experiments			High-NO_x experiments			
OH exposure ($\times 10^{12}$ molecules cm^{-3} s)	Equivalent photochemical age (days)	Background (μg/m^3)	OH exposure ($\times 10^{12}$ molecules cm^{-3} s)	Equivalent photochemical age (days)	Background (μg/m^3)-unseeded	Background (μg/m^3)-seeded
0.05	0.42	0.51	0.08	0.63	0.15	2.74
0.14	1.10	1.55	0.22	1.71	0.33	5.37
0.26	2.00	2.01	0.34	2.64	0.32	6.84
0.35	2.67	2.38	0.45	3.45	0.39	7.44
0.43	3.28	2.25	0.61	4.69	0.37	10.91
0.50	3.86	2.70	0.82	6.36	0.58	12.34
0.60	4.66	3.50	0.90	6.94	0.41	12.21
0.69	5.30	3.73	1.10	8.46	0.98	13.61
0.90	6.95	3.86				
1.16	8.96	5.19				
1.32	10.15	6.17				
1.67	12.88	7.24				
1.85	14.24	7.81				

Table S4. The mass concentrations of D5 SOAs on the basis of effective aerosol density and average SMPS data in the last 10 minutes at different OH exposures under unseeded conditions in low-NO_x experiments.

OH exposure ($\times 10^{12}$ molecules cm^{-3} s)	Equivalent photochemical age (days)	Low-NO_x-unseeded-D5 SOAs ($\mu g/m^3$)
0.05	0.42	0.53
0.14	1.10	2.00
0.26	2.00	9.75
0.35	2.67	18.53
0.43	3.28	28.16
0.50	3.86	53.41
0.60	4.66	75.06
0.69	5.30	106.82
0.90	6.95	185.58
1.16	8.96	250.11
1.32	10.15	277.23
1.67	12.88	309.12
1.85	14.24	299.15

Table S5. Comparison of experimental results and conditions for D5 SOAs in this study with those in other literatures

	D5 SOA yield	Reactor	D5 concentration (ppbv)	SOA concentration (μg m^{-3})	Determination of OH concentration	Determination of reacted precursor	OH concentration (molecules cm^{-3})	OH exposure (molecules cm^{-3} s)	Global average OH concentration (molecules cm^{-3})	Equivalent days	RH (%)	T (˚C)
Wu (2017)	0.08-0.16	photo-oxidation chamber (PC) (50 L)	5.4-13.3	1.2-12	SO_2-OH	Calculation from the OH mixing ratio	10^8	9×10^{10}	—	—	8-10	27
Janechek (2019)	0.22	PAM OFR chamber (13.3 L)	33.14	107.1	SO_2-OH	Solid-phase extraction (SPE) cartridges	—	1.6×10^{12}	1.5×10^6	12.4	25	24
	0.24		24.67	84				2.3×10^{12}		17.4		
	0.24		19.13	68.4				2.7×10^{12}		20.8		
	0.3		48.80	219.7				4.8×10^{12}		37.1	45	
	0.5		24.72	180.7				5.1×10^{12}		39.5		
Charan (2022) (Experiments 1-4: low-NO_x and seeded)	0.015±0.015	Chamber (19 m^3)	497±5	—	Calculated by fitting the gas-phase D5 concentration to a first-order exponential	Gas chromatograph	4.5×10^6	9×10^{10}	—	—	<5	26.6
	0.057±0.08		298±3				3.8×10^6	8×10^{10}				26.5
	0±0.003		30±1				2.2×10^6	6×10^{10}				27.6
	0.026±0.04		580±5				1.6×10^6	3×10^{10}				17.7
Charan (2022) (Experiments 10-15: low-NO_x and unseeded)	0.018±0.002	Caltech Photooxidation Flow Tube (CPOT) (4.88 L)	262±10	—	SO_2-OH	Gas chromatograph	2.3×10^8	1.5×10^{11}	—	—	3	23.0
	0.06±0.006		262±10				5.0×10^8	3.3×10^{11}			4	23.0
	0.046±0.004		262±10				2.3×10^8	1.5×10^{11}			3	23.0
	0.14±0.01		262±10				1.2×10^9	7.8×10^{11}			10	23.0
	0.24±0.02		262±10				1.5×10^9	1.0×10^{12}			16	23.0
	0.35±0.02		262±10				1.6×10^9	1.1×10^{12}			33	23.0
This study	0.02±0.02	ECCC-OFR	18-26	0.5	MeOH-OH	PTR-MS	4.6×10^8	5.5×10^{10}	1.5×10^6	0.4	35	21±1

(Low-NO_x and unseeded)	0.02±0.01	(16 L)		1.8			1.2×10^{9}	1.4×10^{11}		1.1	±2	
	0.11±0.01			16.9			2.9×10^{9}	3.5×10^{11}		2.7		
	0.27±0.03			48.9			4.2×10^{9}	5.0×10^{11}		3.9		
	0.35±0.02			68.7			5.0×10^{9}	6.0×10^{11}		4.7		
	0.46±0.03			97.7			5.7×10^{9}	6.9×10^{11}		5.3		
	0.61±0.03			169.7			7.5×10^{9}	9.0×10^{11}		7.0		
	0.70±0.03			228.8			9.7×10^{9}	1.2×10^{12}		9.0		
	0.75±0.03			253.6			1.1×10^{10}	1.3×10^{12}		10.2		
	0.79±0.03			282.7			1.4×10^{10}	1.7×10^{12}		12.9		
	0.80±0.03			273.6			1.5×10^{10}	1.9×10^{12}		14.2		
This study (Low-NO_x and seeded)	0.02±0.01	ECCC-OFR (16 L)	27-30	0.8	MeOH-OH	PTR-MS	4.6×10^{8}	5.5×10^{10}	1.5×10^{6}	0.4	35 ±2	21±1
	0.01±0.004			2.0			1.2×10^{9}	1.4×10^{11}		1.1		

Table S6. Details about sites and concentrations of cVMS SOAs. The concentrations of cVMS SOAs were calculated on the basis of the cVMS concentrations reported from multiple literatures and SOA yields measured in this work. Here, the chosen concentrations of cVMSs were maximum that have been reported in each site.

Site #	Site Name	Country	Site Type	D3 (ng/m^3)	D3 SOAs (ng/m^3)	D4 (ng/m^3)	D4 SOAs (ng/m^3)	D5 (ng/m^3)	D5 SOAs (ng/m^3)	D6 (ng/m^3)	D6 SOAs (ng/m^3)	Total SOAs (ng/m^3)	References
1	Ny Alesund	Norway	PO	17	0.58	67	0.73	25	0.56	3.8	0.01	1.88	(Genualdi et al., 2011; Rauert et al., 2018)
2	Alert, NU	Canada	PO	13	0.44	72	0.79	26	0.59	39	0.15	1.97	
3	Barrow, AK	USA	PO	1.4	0.05	14	0.15	7.5	0.17	1.1	0.00	0.37	
4	Little Fox Lake, YK	Canada	BA	21	0.72	131	1.43	81	1.83	10	0.04	4.02	
5	West Branch, IA	USA	BA	——	——	14	0.15	29	0.65	2.3	0.01	0.81	(Yucuis et al., 2013)
6	Point Reyes, CA	USA	BA	16	0.54	66	0.72	35	0.79	3.7	0.01	2.06	(Genualdi et al., 2011; Rauert et al., 2018)
7	Hilo, HI	USA	BA	32	1.09	145	1.59	143	3.23	17	0.06	5.97	
8	Bratt's Lake, SK	Canada	BA	17	0.58	100	1.09	44	0.99	5.3	0.02	2.68	
9	Whistler, BC	Canada	BA	117	3.98	45	0.49	10	0.23	1.5	0.01	4.71	
10	Fraserdale, ON	Canada	BA	15	0.51	53	0.58	16	0.36	2.8	0.01	1.46	

11	Ucluelet, BC	Canada	BA	81	2.76	121	1.32	31	0.70	3.5	0.01	4.79	
12	Sable Island, NS	Canada	BA	14	0.48	54	0.59	33	0.74	5.6	0.02	1.83	(Rauert et al., 2018)
13	Mount Revelstoke, BC	Canada	BA	2.4	0.08	30	0.33	33	0.74	9.1	0.03	1.18	(Genualdi et al., 2011; Rauert et al., 2018)
14	Tudor Hill	Bermuda	BA	8	0.27	76	0.83	56	1.26	66	0.25	2.61	
15	Storhofdi	Iceland	BA	3.5	0.12	14	0.15	13	0.29	1.5	0.01	0.57	
16	Malin Head	Ireland	BA	11	0.37	21	0.23	32	0.72	7.4	0.03	1.35	
17	Kosetice	Czech Republic	BA	25	0.85	61	0.67	297	6.70	169	0.64	8.86	
18	Cape Grim	Australia	BA	8.8	0.30	59	0.65	13	0.29	2.4	0.01	1.25	
19	Tibetan Plateau	China	BA	71.1	2.42	96.6	1.06	145.6	3.29	2.9	0.01	6.78	(Wang et al., 2018)
20	Toronto, ON	Canada	UR	18	0.05	77	0.02	247	0.72	22	0.00	0.79	(Krogseth et al., 2013; Ahrens et al., 2014)
21	Chicago, IL	USA	UR	——	——	190	0.04	1100	3.19	50	0.00	3.23	(Yucuis et al., 2013)

22	Cedar Rapids, IA	USA	UR	——	——	37	0.01	65	0.19	9.3	0.00	0.2	(Yucuis et al., 2013)
23	Sydney, FL	USA	UR	10	0.03	76	0.02	93	0.27	6.6	0.00	0.32	(Genualdi et al., 2011; Rauert et al., 2018)
24	Groton, CT	USA	UR	16	0.05	68	0.01	96	0.28	12	0.00	0.34	
25	Boulder, CO	USA	UR	——	——	——	——	65	0.19	——	——	0.19	(Coggon et al., 2018)
26	Zurich	Switzerland	UR	——	——	——	——	650	1.89	79	0.00	1.89	(Buser et al., 2013)
27	Catalan	Spain	UR	1166	3.38	676	0.15	1942	5.63	68	0.00	9.16	(Gallego et al., 2017)
28	Paris	France	UR	30	0.09	50	0.01	280	0.81	53	0.00	0.91	(Genualdi et al., 2011; Rauert et al., 2018)
29	Yantai	China	UR	——	——	22	0.00	38	0.11	——	——	0.11	(Xu et al., 2012)
30	Guangzhou	China	UR	11300	32.80	3300	0.72	——	——	——	——	33.52	(Wang et al., 2001)

31	Macau	China	UR	5800	16.84	4300	0.93	——	——	——	——	17.77	(Wang et al., 2001)
32	Foshan	China	UR	2300	6.68	3500	0.76	——	——	——	——	7.44	(Wang et al., 2001)
33	Dalian	China	UR	——	——	1950	0.42	1440	4.18	990	0.00	4.6	(Li et al., 2020)
34	Kunming	China	UR	——	——	26	0.01	59	0.17	22	0.00	0.18	(Guo et al., 2019)
35	Lhasa	China	UR	44.8	0.13	54.6	0.01	464.6	1.35	1.3	0.00	1.49	(Wang et al., 2018)
36	Golmud	China	UR	26.8	0.08	48.6	0.01	208.1	0.60	2.8	0.00	0.69	(Wang et al., 2018)

Note: '——' means that the data was not obtained for this site; 'PO' means polar sites; 'BA' means background sites; 'UR' means urban sites.

Table S7. The values of $C_{in\text{-}cVMSs}$ and ΔC_{cVMSs} in Equation 4.

cVMSs	Low NO_x-unseeded (14.2 d)		High NO_x-seeded (0.63 d)	
	Initial concentration ($C_{in\text{-}cVMSs}$, μg m^{-3})	Lost concentration (ΔC_{cVMSs}, μg m^{-3})	Initial concentration ($C_{in\text{-}cVMSs}$, μg m^{-3})	Lost concentration (ΔC_{cVMSs}, μg m^{-3})
D3	186.83	156.99	382.32	29.13
D4	386.42	327.30	305.99	54.97
D5	371.66	371.66	569.99	146.54
D6	476.12	453.72	488.59	91.00

References

Ahrens, L., Harner, T., and Shoeib, M.: Temporal Variations of Cyclic and Linear Volatile Methylsiloxanes in the Atmosphere Using Passive Samplers and High-Volume Air Samplers, Environ. Sci. Technol., 48, 9374-9381, https://doi.org/10.1021/es502081j, 2014.

Aiken, A., Decarlo, P., and Jimenez, J.: Elemental Analysis of Organic Species with Electron Ionization High-Resolution Mass Spectrometry, Anal. Chem., 79, 8350-8358, https://doi.org/10.1021/ac071150w, 2007.

Buser, A., Kierkegaard, A., Bogdal, C., MacLeod, M., Scheringer, M., and Hungerbühler, K.: Concentrations in Ambient Air and Emissions of Cyclic Volatile Methylsiloxanes in Zurich, Switzerland, Environ. Sci. Technol., 47, 7045-7051, https://doi.org/10.1021/es3046586, 2013.

Charan, S., Huang, Y., Buenconsejo, R., Li, Q., Cocker Iii, D., and Seinfeld, J.: Secondary Organic Aerosol Formation from the Oxidation of Decamethylcyclopentasiloxane at Atmospherically Relevant OH Concentrations, Atmos. Chem. Phys., 22, 917-928, https://doi.org/10.5194/acp-22-917-2022, 2022.

Coggon, M., McDonald, B., Vlasenko, A., Veres, P., Bernard, F., Koss, A., Yuan, B., Gilman, J., Peischl, J., Aikin, K., DuRant, J., Warneke, C., Li, S.-M., and Gouw, J.: Diurnal Variability and Emission Pattern of Decamethylcyclopentasiloxane (D5) from the Application of Personal Care Products in Two North American Cities, Environ. Sci. Technol., 52, 5610-5618, https://doi.org/10.1021/acs.est.8b00506, 2018.

Gallego, E., Perales, J., Roca, F., Guardino, X., and Gadea, E.: Volatile Methyl Siloxanes (VMS) Concentrations in Outdoor Air of Several Catalan Urban Areas, Atmos. Environ., 155, 108-118, http://dx.doi.org/10.1016/j.atmosenv.2017.02.013, 2017.

Genualdi, S., Harner, T., Cheng, Y., Macleod, M., Hansen, K., Egmond, R., Shoeib, M., and Lee, S.: Global Distribution of Linear and Cyclic Volatile Methyl Siloxanes in Air, Environ. Sci. Technol., 45, 3349-3354, https://doi.org/10.1021/es200301j, 2011.

Guo, J., Zhou, Y., Cui, J., Zhang, B., and Zhang, J.: Assessment of Volatile Methylsiloxanes in Environmental Matrices and Human Plasma, Sci. Total. Environ., 668, 1175-1182, https://doi.org/10.1016/j.scitotenv.2019.03.092, 2019.

Janechek, N., Marek, R., Bryngelson, N., Singh, A., Bullard, R., Brune, W., and Stanier, C.: Physical Properties of Secondary Photochemical Aerosol from OH Oxidation of a Cyclic Siloxane, Atmos. Chem. Phys., 19, 1649-1664, https://doi.org/10.5194/acp-19-1649-2019, 2019.

Krogseth, I., Zhang, X., Lei, Y., Wania, F., and Breivik, K.: Calibration and Application of a Passive Air Sampler (XAD-PAS) for Volatile Methyl Siloxanes, Environ. Sci. Technol., 47, 4463-4470, https://doi.org/10.1021/es400427h, 2013.

Li, Q., Lan, Y., Liu, Z., Wang, X., Wang, X., Hu, J., and Geng, H.: Cyclic Volatile Methylsiloxanes (cVMSs) in the Air of the Wastewater Treatment Plants in Dalian, China-Levels, Emissions, and Trends, Chemosphere, 256, 1-8, https://doi.org/10.1016/j.chemosphere.2020.127064, 2020.

Rauert, C., Shoieb, M., Schuster, J., Eng, A., and Harner, T.: Atmospheric Concentrations and Trends of Poly- and Perfluoroalkyl Substances (PFAS) and Volatile Methyl Siloxanes (VMS) over 7 Years of Sampling in the Global Atmospheric Passive Sampling (GAPS) Network, Environ. Pollut., 238, 94-102, https://doi.org/10.1016/j.envpol.2018.03.017, 2018.

Wang, X., Schuster, J., Jones, K., and Gong, P.: Occurrence and Spatial Distribution of Neutral Perfluoroalkyl Substances and Cyclic Volatile Methylsiloxanes in the Atmosphere of the Tibetan Plateau, Atmos. Chem. Phys., 18, 8745-8755, https://doi.org/10.5194/acp-18-8745-2018, 2018.

Wang, X., Lee, S., Sheng, G., Chan, L., Fu, J., Li, X., Min, Y., and Chan, C.: Cyclic organosilicon compounds in ambient air in Guangzhou, Macau and Nanhai, Pearl River Delta, Appl. Geochemistry, 16, 1447-1454, https://doi.org/10.1016/S0883-2927(01)00044-0, 2001.

Wu, Y. and Johnston, M.: Aerosol Formation from OH Oxidation of the Volatile Cyclic Methyl Siloxane (cVMS) Decamethylcyclopentasiloxane, Environ. Sci. Technol., 51, 4445-4451, https://doi.org/10.1021/acs.est.7b00655, 2017.

Xu, L., Shi, Y., Wang, T., Dong, Z., Su, W., and Cai, Y.: Methyl Siloxanes in Environmental Matrices around a Siloxane Production Facility, and Their Distribution and Elimination in Plasma of Exposed Population, Environ. Sci. Technol., 46, 11718-11726, https://doi.org/10.1021/es3023368, 2012.

Yucuis, R., Stanier, C., and Hornbuckle, K.: Cyclic Siloxanes in Air, Including Identification of High Levels in Chicago and Distinct Diurnal Variation, Chemosphere, 92, 905-910, https://doi.org/10.1016/j.chemosphere.2013.02.051, 2013.